Netsu Sokutei **22** (4) 203-211

解　説

The Effect of the Water Vapor Pressure on the Kinetics of the Thermal Dehydration of Some Hydrates. Examples of Magnesium, Manganese, Cobalt, Zinc, Yttrium and Erbium Formate Dihydrates

Yoshio Masuda

(Received March 29, 1995)

The effect of water vapor pressure on the kinetics of the thermal dehydration of some formate hydrates was studied by means of isothermal gravimetry under various water vapor pressures from 6.7×10^{-2} to 1.33×10^{3} Pa. The rates of dehydrations of Zn, Y and Er formate dihydrates exhibited an unusual dependence upon the water vapor pressure; with increasing water vapor pressure the rates increased at first, passed through a maximum, and then decreased gradually to a constant values. These unusual phenomena were analogous to the Smith-Topley effect. On the other hand, the rates of dehydrations of Mg, Mn and Co formate dihydrates decreased with increasing water vapor pressure as was naturally expected from the equilibrium theory.

The mechanism of the unusual phenomena was discussed in correlation with the crystallinity of the dehydrated products.

Introduction

Crystalline hydrates can not be distinguished from other solid reactants on chemical or structural criteria, however, the considerable interest which has been directed towards investigation of the dehydrations of this group, has made it convenient to discuss them as a single class.[1] Generally, dehydrations are reversible reaction and influenced by the product phase on the ease of water escape, because such residual material tends to greater or lesser extent, to diminish the rate of diffusion of water from the reaction interface. It has been also known that the rate of thermal dehydration of hydrate is affected by the atmospheric water vapor pressure.

The phenomenon of an unusual variation in the dehydration rate with the partial pressure of water vapor was noted by Smith and Topley.[2,3] They reported that the rate constants for the dehydration of manganese oxalate dihydrate and copper sulfate pentahydrate vary unusually with the partial pressure of atmospheric water vapor. When water vapor pressure is increased, the rate constant for the dehydration decreases sharply at first, pass through a minimum, increases more slowly, and then decreases (**Fig.1**). This unusual phenomenon is known as the Smith-Toply effect. Gerner *et al.* have made similar studies of copper sulfate pentahydrate and

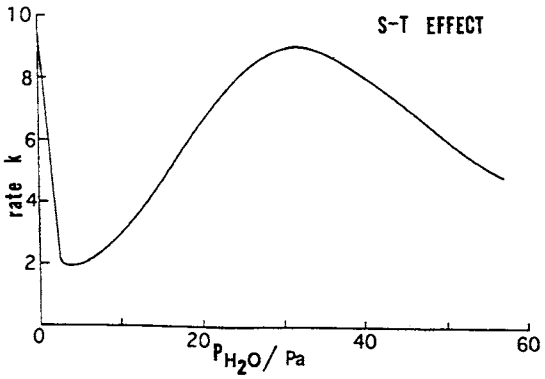

Fig.1 Schematic representation of Smith-Topley (S-T) effect.

Department of Environmental Science, Faculty of Science, Niigata University, Ikarashi -2, Niigata 950-21, Japan

potassium anmmonium chrome alum.[4-5] Recently similar phenomenon has also been observed by Dollimore et al. on the dehydrations of calcium oxalate monohydrate and magnesium oxalate dihydrate.[6-7] The effect, however, has not been always recognized in all dehydration.

Although no single mechanistic explanation has been accepted as possessing general validity, several mechanistic models have been proposed as follows [8] : (1) properties of adsorbed water,[3,9,10] (2) recrystallization of product phase [1,11-14] and (3) heat and gas transfer at the reaction and interface.[15,16] It may be possible that concurrent or intermediate behavior of these models and different mechanism may operate for different solid.

We have also found that similar phenomena to the Smith-Topley effect occurred on the dehydrations of some formate hydrates.[17-19] In the present paper, the mechanism of the phenomenon is discussed briefly on the basis of the crystallinity of the dehydrated product phase.

Experimental

Reagents; magnesium, manganese, cobalt, zinc and yttrium formate dihydrates were obtained commercially and recrystallized from distilled water. Erbium formate dihydrate was prepared by the reaction of formic acid and erbium oxide as follows. Erbium oxide purchased from Shin-Etsu Chemical Co. Ltd., Japan, was combined with a large excess of aqueous formic acid solution. The mixture was held with stirring at the temperature just below its boiling point until the oxide had dissolved. The crystals of erbium formate dihydrate were obtained by slow evaporation of the solution and kept in a desiccator.

These samples were pulverized with a mortar and pestle, and sieved to a fraction 80 - 150 mesh size.

Apparatus; Two experimental methods have been used to study the kinetics of the thermal reactions of solid, mainly, dynamic method and isothermal method. Each of methods has advantage and disadvantage. [8,20,21] In this paper, the isothermal method was adopted to study the kinetics of the thermal dehydrations of the titled hydrates, and the dehydration process was followed using a Shinku Riko TGD-5000RH differential microbalance equipped with an infrared gold image furnace.[17-19,22,23] A sample of about 5 mg was weighed into platinum crucible and placed in the microbalance. The furnace was controlled at given temperatures and maintained within ±0.5 ℃ until the dehydration was completed. The TG output voltages were amplified and recorded on a microcomputer (Epson QC－10II) via A/D converter (Datel-Intersil 7109 modified to 13 bit) .[17-19,22,23] About 1000 data points were collected at a given time intervals for each dehydration process, and the fraction of dehydration, α was calculated from these data.

The water vapor pressure of the reaction system was regulated from 6.7×10^{-2} to 1.3×10^{3} Pa according to the following procedure. The reaction system was degassed for 3 - 4 h before experiment, to below 6.7×10^{-2} Pa, and a suitable amount of water vapor was then admitted from a water bulb which was maintained at a constant temperature to provide a constant vapor pressure.[17-19]

X-ray powder diffraction patterns were obtained with a Rigaku Geiger-flex RAD-γA and a RAD 3R diffractometers equipped with a standard high temperature sample holder. Cu Kα radiation, a nickel filter and a graphite monochrometer were used for all measurements. The diffraction data were collected at 0.02° intervals.

Results and Discussion

The smoothness of the TG and DTA curves of these hydrates and agreement between the calculated and observed weight loss suggest that dehydrations proceed successively without any intermediate such as the mono-

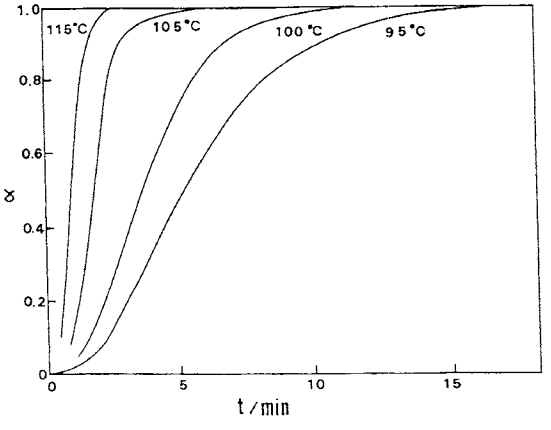

Fig.2 Typical α vs. t plots for the thermal dehydration of zinc formate dihydrate.

Table 1 Commonly used g(α) for solid phase reaction.

$g(\alpha)$	Symbol	Rate-controlling process
α^2	D_1	One-dimensional diffusion
$\alpha+(1-\alpha)\ln(1-\alpha)$	D_2	Two-dimensional diffusion
$(1-(1-\alpha)^{1/3})^2$	D_3	Three-dimensional diffusion ; Jander Equiation
$1-2\alpha/3-(1-\alpha)^{2/3}$	D_4	Three-dimensional diffusion ; Ginstring-Brounshtein equiation
$1-(1-\alpha)^{1/2}$	R_2	Two-dimensional phase boundary reaction
$1-(1-\alpha)^{1/3}$	R_3	Three-dimensional phase boundary reaction
$-\ln(1-\alpha)$	F_1	First-order reaction
$[-\ln(1-\alpha)]^{1/m}$	A_m	Avrami-Erofe'ev equation, m=1, 2, 2.5, 3, ...

hydrate for all of the dihydrates. **Fig.2** shows a typical plot of the dehydration fraction, α for the dehydration of zinc formate dihydrate, against the reaction time, *t*. These dehydration data were analyzed by means of integral method as follows.

The rate of dehydration can be expressed by

$$d\alpha/dt = kf(\alpha) \quad \cdots\cdots (1)$$

where α is the dehydration fraction after time *t*, *k* is the rate constant, and $f(\alpha)$ is a function depending on the dehydration mechanism and the geometry of the reacting particles. The eq. (1) can be converted to the integrated form

$$g(\alpha) \equiv \int d(\alpha)/f(\alpha) = \int k\,dt = kt \quad \cdots\cdots (2)$$

where $g(\alpha)$ is the function depending on the dehydration mechanism as well as $f(\alpha)$. **Table 1** shows the theoretical model function used commonly.[24-28] The $g(\alpha)$ of the present dehydrations were determined by the linearity of the plots of various $g(\alpha)$ against *t* in accordance with eq. (2).

1) Thermal dehydrations of magnesium, manganese, cobalt and zinc formate dihydrate.

The $g(\alpha)$ function determined for the these dehydrations tend to vary with atmospheric water vapor pressure, *i.e.* at lower vapor pressure the dehydration seems to be described by

$$[-\ln(1-\alpha)]^{1/2} = kt \quad \cdots\cdots (3)$$

which is referred to as an Avrami-Erofeev equation (A_2), but at the region of the vapor pressure higher than 52 Pa, it confirms with a two-dimensional phase boundary controlled reaction (R_2) (**Fig.3**).

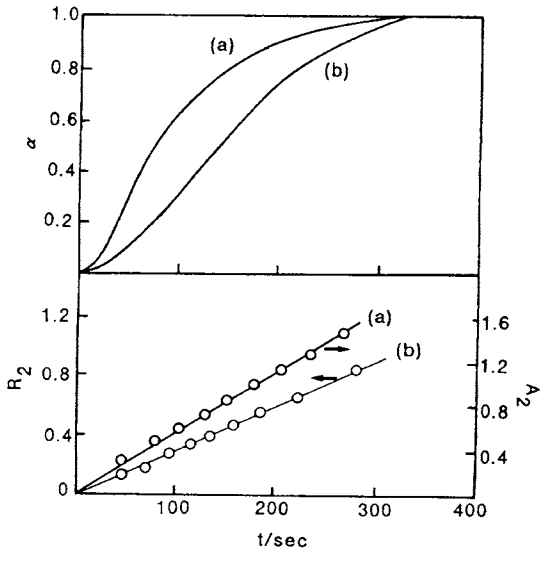

Fig.3 Typical α vs. *t* and $g(\alpha)$ vs. *t* plots for the dehydration of $Zn(HCO_2)_2 \cdot 2H_2O$: (a) at 100 ℃, 16 Pa of water vapor pressure; (b) at 100 ℃, 530 Pa of water vapor pressure.

$$1-(1-\alpha)^{1/2} = kt \quad \cdots\cdots (4)$$

However, the plot of $1-(1-\alpha)^{1/2}$ vs. *t* (*i.e.* plot of R_2 vs. *t*) gave a relatively straight line over the wide range of the water vapor pressures.

An R_2 is characterized by rapid initial production of a complete reactant-product interface at the edge of preferred crystallographic surface, and its rate is depend upon the advance of this reaction interface.[24-28] **Fig.4**

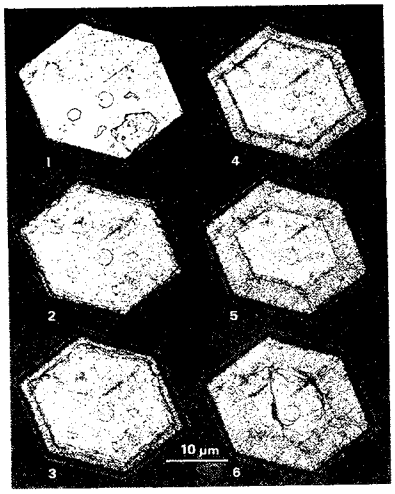

Fig.4 Optical microscopic observations of the dehydration of $Zn(HCO_2)_2 \cdot 2H_2O$ at 1.7×10^3 Pa of water vapor pressure : 1, crystal of a hydrated specimen; 2, after heating for 2.5 min at 108 ℃; 3, after heating for 3 min at 108 ℃; 4, after heating for 3.5 min at 108 ℃; 5, after heating for 4.5 min at 108 ℃; 6, after heating for 7 min at 108 ℃.

shows the advance of the dehydration interface of zinc formate dihydrate. The series of photographs shows that an interface is immediately established at the edge of the disc, and then advances into the center. The rate of advance of the interface, which was directly determined from the micrographs, agreed with that obtained from thermogravimetry within experimental error.[23]

The R_2 mechanism for the present dehydration is supported by consideration of the crystal structure of these hydrates reported by several investigators.[29-31] They showed that these hydrates form isomorphous crystals, and the crystal structure is monoclinic with space group P21/c. In this structure, the unit cell includes two metallic ions. One of the metallic ions is surrounded by six carbonyl oxygen atoms, the other is surrounded by two carbonyl oxygen atoms and four water molecules. Both are in a regular octahedral form, with the water molecule lying on a plane parallel to the (100) planes. It is reasonable to consider that the dehydration takes place on these plane. The kinetics of dehydrations of the other hydrates of these series can be described by similar equation, R_2.

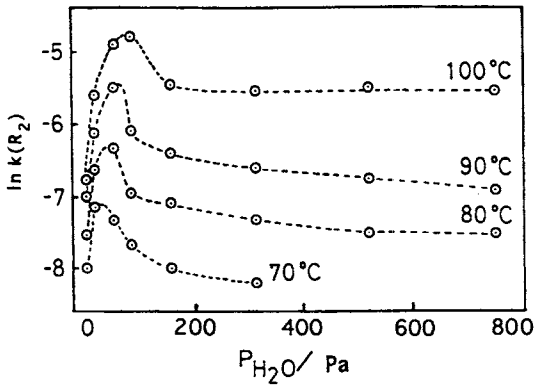

Fig.5 Variation of dehydration rate, k for the dehydration of $Zn(HCO_2)_2 \cdot 2H_2O$ with water vapor pressure.

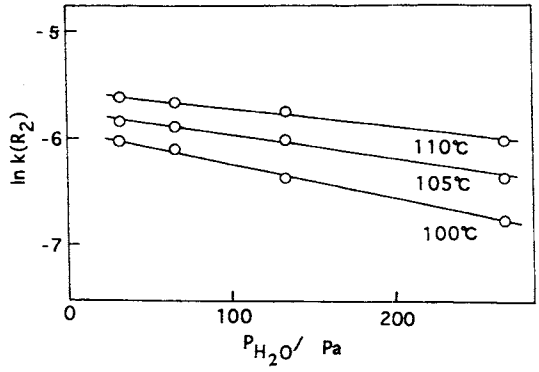

Fig.6 Variation of dehydration rate, k for the dehydration of $Mg(HCO_2)_2 \cdot 2H_2O$ with water vapor pressure.

Fig.5 shows the relations between the rate of dehydration, k and the water vapor pressure at particular temperatures. The values of k increased with increasing of water vapor pressure, reached to a maximum, and then decreased gradually to a constant value. When these results are compared with the Smith-Topley phenomenon, they are lacking the initial decreasing region of k at low water vapor pressure, however, these results are similar to the Smith-Topley effect. On the other hand, the similar phenomenon to the Smith-Topley effect was not found for the dehydrations of Mg,[32] Mn,[33] and Co[34] formate dihydrates (**Figs.6** and **7**, and **Table 2**)

X-ray diffraction profiles indicated that the anhydrous zinc formate formed in vacuum was amorphous, while

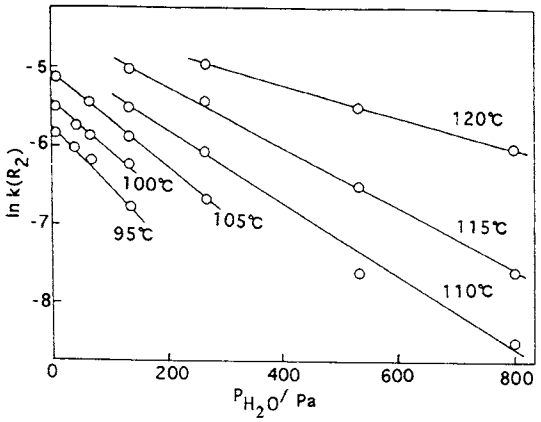

Fig.7 Variation of dehydration rate, k for the dehydration of $Co(HCO_2)_2 \cdot 2H_2O$ with water vapor pressure.

Table 2 The velocity of the interface advancing, k_j for the dehydration of $Mn(HCO_2)_2 \cdot 2H_2O$.

	$kj/cm \cdot s^{-1}$			
	$T/℃$			
P_{H_2O}/Pa	95	100	105	110
6.13×10^2	0.98	1.83	3.36	6.09
8.93×10^2	0.66	1.26	2.37	4.39
1.38×10^3	0.61	1.18	2.24	4.18

that formed in self-generated atmospheric water vapor pressure was crystalline (**Fig.8**) . These findings show that the crystalline anhydride seems to form at above a critical water vapor pressure. The critical temperatures for the zinc formate are illustrated in **Fig.9**. The temperatures decreased linearly with increasing critical water vapor pressure. These facts indicate the availability of atmospheric water molecules to form a crystalline zinc formate.

It should be noted that the dehydration takes place as an A_2 reaction at below critical water vapor pressures and temperatures, but as an R_2 reaction at above critical values. The unusual phenomena shown in **Fig.5** may also be related to the crystallinity of the dehydrated product. This seems to be supportable by the experimental fact that the dehydration was described by the A_2 equation especially at low temperature. The equation A_2 is the kinetic expression concerning with the random nu-

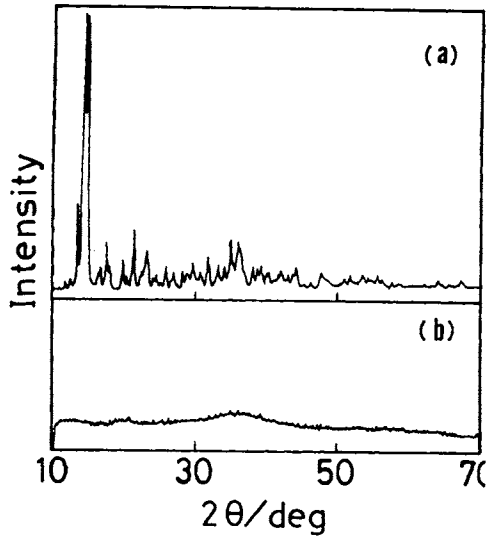

Fig.8 X-ray powder diffraction profiles of $Zn(HCO_2)_2 \cdot 2H_2O$:
(a) dehydrated at 95 ℃ and 93 Pa of water vapor pressure;
(b) dehydrated at 95 ℃ in vacuum ($\sim 1.3 \times 10^{-1}$ Pa)

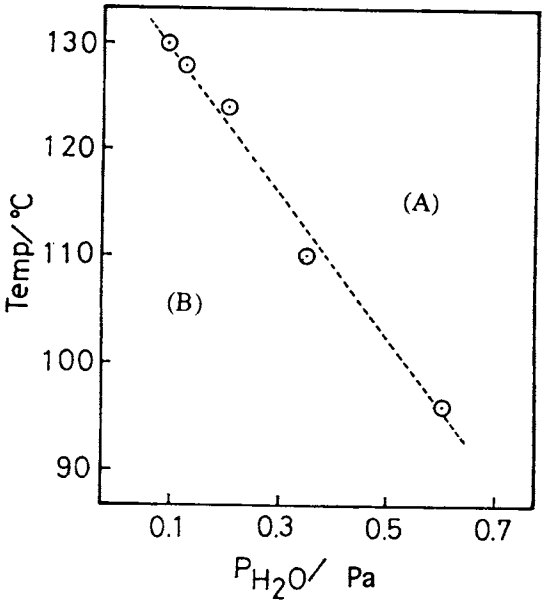

Fig.9 Relation between the critical temperature and the critical water vapor pressure at which crystalline zinc formate formed : (A) shows the region of crystalline product; (B) shows the region of amorphous product.

cleation and nuclei growth process. Hulbert pointed out the relation between the nuclei growth and the diffusion process of migrating species as follows : [25] when (i) the nucleation rate is assumed to be constant, (ii) the nuclei grow two-dimensionally and (iii) the growth is diffusion controlled, eq. (3) can be derived on the basis of the overall rate constant to be given by eq. (5)

$$k = (\pi hID/2)^{1/2} \quad \cdots\cdots (5)$$

where I is the nucleation rate per unit volume, h is the thickness of the sample, and D is the diffusion coefficient of the migrating species. On the basis of above opinion, the reaction described by the A_2 would be controlled by the diffusion process of the migrating species *i.e.*, in the present dehydration, the rate would be controlled by the diffusion of the dissociated water molecules though the amorphous phase, at a low water vapor pressures, especially at low temperature.

At low water vapor pressure, the amorphous products of zinc formate may adsorb the dissociated water molecules. This would interfere with the escape of further water molecules, and the rate of dehydration would therefore be slow. The presence of a few water vapor molecules stimulates crystallization of the dehydrated products. The initial increase in the value of k suggests that recrystallization may bring about the formation of wide channels between the dehydrated particles, through which the dissociated water molecules are able to escape. The value of k would therefore seem to increase at first.

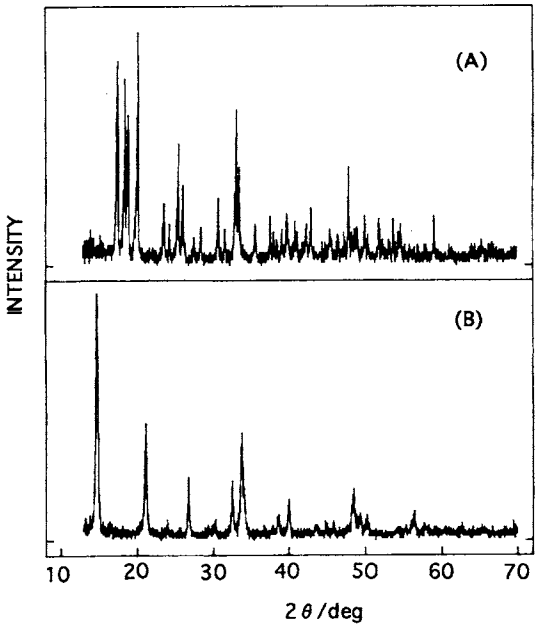

Fig.10 X-ray powder diffraction profiles of manganese formate dihydrate (A), and the dehydrated product (B) formed at 150℃ in vacuum.

At high vapor pressure, however, the apparent rate of dehydration decreases gradually because of the reverse reaction caused by atmospheric water molecules. On the other hand, the similar phenomena to the Smith-Topley effect were not recognized for the dehydrations of Mg, Mn and Co formate dihydrates. In these dehydrations, the crystalline dehydrates were formed both in vacuum (**Fig.10**) and in self-generated atmospheric water vapor pressure. These facts seem to support above opinion for the mechanism of the Smith-Topley phenomenon.

2) Yttrium formate dihydrate and rubidium formate dihydrate.

These hydrates have a similar crysrallographic structure [35,36] and the kinetic behavior of the dehydration also resemble to each other. The $g(\alpha)$ functions selected tend to vary with atmospheric water vapor pressure (**Tables 3** and **4**). At low vapor pressure ($\sim 6.7 \times 10^{-2}$ Pa) and especially low temperatures, the initial stages of these dehydrations seem to be described by an Avrami-Erofeev equation, A_2.

$$[-\ln(1-\alpha)]^{1/2} = kt \quad \cdots\cdots (6)$$

However, in the main stages of the dehydrations can be described as a three-dimensional phase boundary reaction, R_3, *i.e.*

$$1-(1-\alpha)^{1/3} = kt \quad \cdots\cdots (7)$$

The R_3 reaction has been characterized by the rapid initial production of a complete reactant-product interface at the surface of reactant particles, and its rate is determined by the advance of the reaction interface to the center of the particles.

Figures 11 and **12** show the relation between the rate of dehydration, k and the water vapor pressure at particular temperatures. The values of k increased with in-

Table 3 Variation of $g(\alpha)$ for the dehydration of $Y(HCO_2)_3 \cdot 2H_2O$ with the atomospheric water vapor pressure.

P_{H_2O}/Pa	T/℃	$G(\alpha)$	Range of α	C*	ln k
6.7×10^{-2}	114	A_2	0.131-0.442	0.9990	−8.30
		R_3	0.550-0.980	0.9995	−8.19
	124	A_2	0.014-0.263	0.9990	−7.67
		R_3	0.413-0.825	0.9991	−7.74
	134	A_2	0.014-0.203	0.9964	−7.13
		R_3	0.440-0.950	0.9980	−6.93
1.33×10^{-2}	114	A_2	0.094-0.376	0.9993	−8.50
		R_3	0.452-0.927	0.9998	−8.52
	124	R_3	0.058-0.925	0.9995	−7.50
	134	R_3	0.020-0.987	0.9999	−5.90
6.66×10^{-2}	114	R_3	0.025-0.895	0.9990	−9.25
	124	R_3	0.015-0.971	0.9997	−7.80
	134	R_3	0.010-0.905	0.9999	−6.19

* correlation coefficient

Table 4 Variation of $g(\alpha)$ for the dehydration of $Er(HCO_2)_3 \cdot 2H_2O$ with the atomospheric water vapor pressure.

P_{H_2O}/Pa	T/℃	$G(\alpha)$	Range of α	C*	ln k
6.7×10^{-2}	104	R_3	0.289-0.885	0.9995	−9.50
		A_2	0.061-0.802	0.9996	−8.71
	114	R_3	0.373-0.966	0.9996	−8.26
		A_2	0.008-0.531	0.9994	−7.98
	124	R_3	0.368-0.818	0.9985	−7.35
		A_2	0.011-0.541	0.9977	−7.55
	144	R_3	0.197-0.528	0.9955	−6.76
		A_2	0.083-0.533	0.9989	−5.80
6.7×10^{-3}	114	R_3	0.189-0.881	0.9996	−8.58
		A_2	0.029-0.551	0.9997	−7.81
	119	R_3	0.095-0.561	0.9996	−6.82
		A_2	0.058-0.355	0.9977	−6.31
	124	R_3	0.020-0.776	0.9998	−5.96
		A_2	0.195-0.690	0.9997	−5.12
	134	R_3	0.190-0.910	0.9996	−5.34
1.33×10^{2}	114	R_3	0.268-0.923	0.9999	−8.71
		A_2	0.031-0.343	0.9963	−6.85
	124	R_3	0.158-0.706	0.9944	−6.60
		A_2	0.028-0.290	0.9987	−5.08
	134	R_3	0.191-0.803	0.9987	−5.24
	143	R_3	0.063-0.925	0.9990	−4.78
1.07×10^{3}	119	R_3	0.101-0.635	0.9995	−8.07
	124	R_3	0.094-0.705	0.9999	−7.06
	134	R_3	0.081-0.735	0.9998	−5.73
	144	R_3	0.081-0.925	0.9999	−5.17

* Correlation coefficient

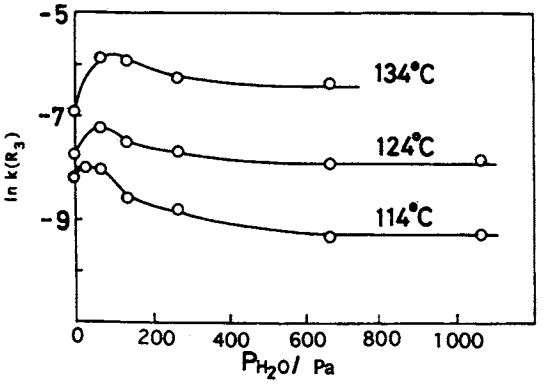

Fig.11 Variation of dehydration rate, k for the dehydration of $Y(HCO_2)_3 \cdot 2H_2O$ with water vapor pressure.

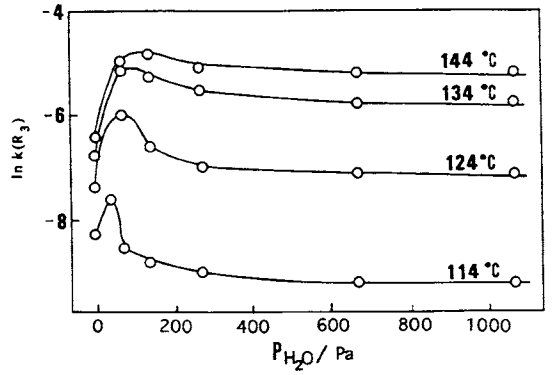

Fig.12 Variation of dehydration rate, k for the dehydration of $Er(HCO_2)_3 \cdot 2H_2O$ with water vapor pressure.

creasing of water vapor pressure, reached to a maximum values, and decreased gradually to a constant values. These phenomena are analogous to the Smith-Topley effect and are also observed previously in the case of thermal dehydration of zinc formate dihydrate.

The X-ray diffraction profiles show that the anhydrous formates formed in vacuum were amorphous (**Figs. 13** and **14**), while those formed in the self-generated atmosphere was crystalline. From these results, the mechanism of the unusual phenomena shown in **Figs. 11** and **12** can be interpreted in a similar way as the case of the dehydration of zinc formate dihydrate.

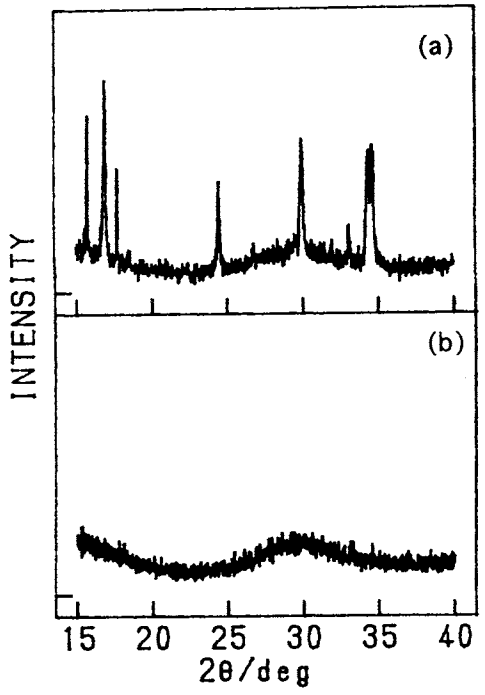

Fig.13 X-ray powder diffraction profiles of $Y(HCO_2)_3 \cdot 2H_2O$:

(a) dehydrated at 123 ℃ in the self-generated atmosphere;

(b) dehydrated at 117 ℃ in vacuum ($\sim 1.3 \times 10^{-1}$ Pa)

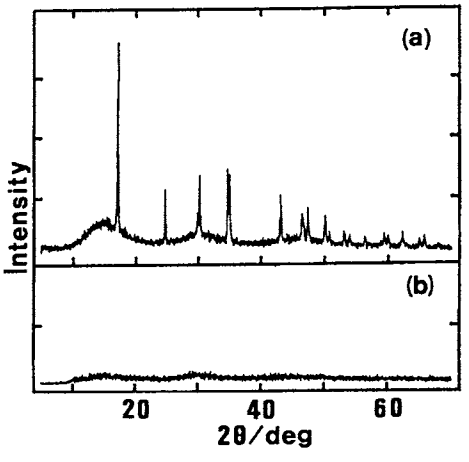

Fig.14 X-ray powder diffraction profiles of $Er(HCO_2)_3 \cdot 2H_2O$:

(a) dehydrated at 115 ℃ and water vapor press of 2×10^3 Pa.

(b) dehydrated at 115 ℃ in vacuum ($\sim 6.2 \times 10^{-2}$ Pa).

Acknowledgement

The present work was supported by a Grant-in-Aid for Scientific Research on Priority Areas "New Development of Rare Earth Complexes" No.07230230 from The Ministry of Education, Science and Culture.

References

1) W. E. Garner (Ed.), Chemistry of the Solid State, Butterworth, London, 1955, p. 213.
2) M. L. Smith and B. Topley, *Proc. Roy. Soc. London Ser. A* **134**, 224 (1931).
3) B.Topley and M. L. Smith, *J. Chem. Soc.* **321** (1935).
4) W. E. Garner and M. G. Tanner, *J. Chem. Soc.* **47** (1930).
5) W. E. Garner and T. S. Jennings, *Proc. Roy. Soc. London Ser. A* **224**, 460 (1954).
6) D. Dollimore, T .E. Jones and P .Spooner, *J. Chem. Soc. Ser. A*, 2809 (1970).
7) D. Dollimore, G. R. Heal and J. Mason, *Thermochim. Acta* **24**, 307 (1978).
8) W .E. Brown, D. Dollimore and A. K. Gallway, in C. H. Bamford and C. F. H. Tipper (Eds.), Comprehensive Chemical Kinetics, Vol.22 : Reactions in the Solid State, Elsevier, Amsterdam, 1980, p.1
9) N. Z. Lyakhov, V. V. Boldyrev and V. P. Isupov, *Kinet. Katal.* **15**, 1224 (1974).
10) G. Thomas, J. J. Gardet, J. J. Gruffat, B. Guihot and M. Soustelle, *J. Chim. Phys.* **69**, 375 (1972).
11) M. Volmer and G. Seydel, *Z. Phys. Chem.* **179**, 153 (1937).
12) R. C. Eckhardt and T. B. Flanagan, *Trans. Faraday Soc.* **60**, 1289 (1964).
13) P. M. Fichte and T. B. Flanagan, *Trans. Faraday Soc.* **67**, 1467 (1971).
14) T. A. Clarke and J. M. Thomas, *J. Chem. Soc. Ser. A*, 2227, 2230 (1969).
15) G. Bertrand, M. Lallemant and G. Watelle-Marion, *J. Inorg. Nucl. Chem.* **36**, 1303 (1974).
16) G. Bertrand, M. Lallemant, A. Mokhlisse and G. Watelle-Marion, *J. Inorg. Nucl. Chem.* **40**, 819 (1978).
17) Y. Masuda and K. Nagagata, *Thermochim. Acta*, **155**, 255 (1989).
18) Y. Masuda and Y. Ito, *J. Thermal Anal.* **38**, 1793 (1992).
19) Y. Masuda, K. Hirata and Y. Ito, *Thermochim. Acta* **203**, 289 (1992).
20) W. E. Garner (Ed.), *Chemistry of the Solid State, Butterworth, London*, 1955, Chap. 7.
21) J. Sestak, V. Satava and W. W. Wendlandt, *Thermochim. Acta* **7**, 333 (1973).
22) Y. Masuda, K. Iwata, R. Ito and Y. Ito, *J. Phys. Chem.* **91**, 6543 (1987).
23) Y. Masuda and K. Nagagata, *Themochim. Acta* **161**, 55 (1990).
24) J. H. Sharp, G. W. Brindley and B. N. N. Achar, *J. Am. Ceram. Soc.* **49**, 379 (1966).
25) S. F. Hulbert, *J. Brit. Ceram. Soc.* **6**, 11 (1969).
26) J. Sestak and G.Berggren, *Thermochim. Acta* **3**, 1 (1971).
27) K. Heide, W. Höland, H. Gölker, K. Seyfarth, B. Müller and R. Sauer, *Thermochim. Acta* **13**, 365 (1975).
28) M.E. Brown, Introduction to Thermal Analysis, Chapmann & Hall, 1988, p.127.
29) K. Krogmann and R. Mattes, *Z. Kristallogr.* **118**, 291 (1963).
30) K. Osaki, Y. Nakai and T. Watanabe, *J. Phys. Soc. Jpn.* **18**, 919 (1963).
31) T. Ogata, T. Taga and K. Osaki, Bull. *Chem. Soc. Jpn.* **50**, 1674 (1977).
32) 長潟和夫, 伊藤良夫, 増田芳男, 第25回熱測定討論会講演要旨集, 1989, (大阪), p.120.
33) Y. Masuda and K. Iwata, *J. Thermal Anal.* **44**, 1013 (1995).
34) 長潟和夫, 伊藤良夫, 増田芳男, 支部合同新潟地方大会講演要旨集, 1989, (長岡), p.126.
35) A. Pabst, Canad. *Mineral.* **16**, 437 (1978).
36) H. R. Wenk, *Z. Kristallogr.* **154**, 137 (1981).

要　旨

ギ酸マグネシウム, マンガン, コバルト, 亜鉛, イットリウムおよびエルビウム2水和物の脱水反応の速度を定温TG法によって測定して, これに対する雰囲気水蒸気圧の影響を精査した。亜鉛, イットリウムおよびエルビウム塩水和物の脱水反応ではSmith-Topley効果に類似した現象, すなわち, 雰囲気水蒸気圧の増加とともに反応速度は増大し, 極大値を経た後に緩やかに減少する傾向が観察された。しかし, 本研究で取り扱った他の水和物ではこの現象は認められなかった。この現象の原因を, 脱水反応によって生成される無水物の結晶性と関係づけて考察した。